JACC: BASIC TO TRANSLATIONAL SCIENCE VOL. 5, NO. 4, 2020

PRECLINICAL RESEARCH

Therapeutic Antibody Against Phosphorylcholine Preserves Coronary Function and Attenuates Vascular ^{18}F-FDG Uptake in Atherosclerotic Mice

Mia Ståhle, MSc,[a] Johanna M.U. Silvola, PhD,[a] Sanna Hellberg, PhD,[a] Margreet de Vries, PhD,[b] Paul H.A. Quax, PhD,[b] Jeffrey Kroon, PhD,[c] Petteri Rinne, PhD,[d,e] Alwin de Jong, MSc,[b] Heidi Liljenbäck, MSc,[a,e] Nina Savisto, PhD,[a] Anna Wickman, PhD,[f] Erik S.G. Stroes, MD, PhD,[c,g] Seppo Ylä-Herttuala, MD, PhD,[h] Pekka Saukko, MD, PhD,[i] Tommy Abrahamsson, MD, PhD,[j] Knut Pettersson, PhD,[j] Juhani Knuuti, MD, PhD,[a,k] Anne Roivainen, PhD,[a,e] Antti Saraste, MD, PhD[a,k,l,m]

VISUAL ABSTRACT

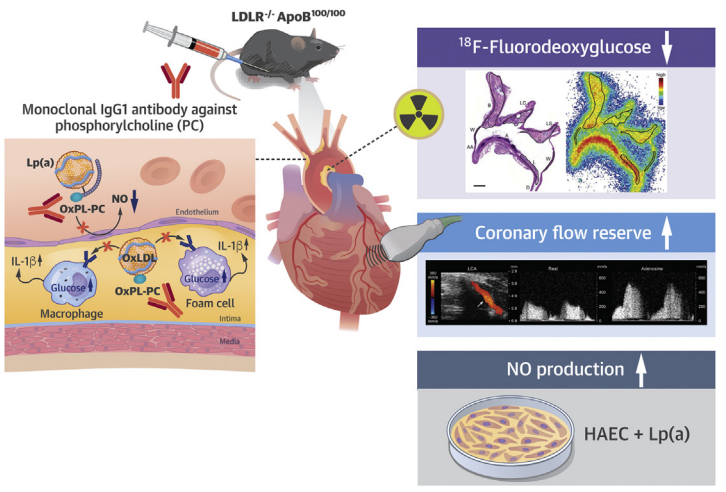

Ståhle, M. et al. J Am Coll Cardiol Basic Trans Science. 2020;5(4):360–73.

HIGHLIGHTS

- **Phosphorylcholine is a pro-inflammatory epitope in atherogenic oxidized phospholipids.**
- **This study investigated effects of a novel monoclonal IgG1 antibody against PC on vascular function and atherosclerotic inflammation.**
- **Treatment with phosphorylcholine antibody preserved coronary flow reserve and decreased uptake of ^{18}F-FDG in atherosclerotic lesions in hypercholesterolemic mice.**
- **Noninvasive imaging techniques represent translational tools to assess the efficacy of phosphorylcholine-targeted therapy on coronary artery function and atherosclerosis.**

ISSN 2452-302X https://doi.org/10.1016/j.jacbts.2020.01.008

SUMMARY

This study showed that treatment with a therapeutic monoclonal immunoglobulin-G1 antibody against phosphorylcholine on oxidized phospholipids preserves coronary flow reserve and attenuates atherosclerotic inflammation as determined by the uptake of ^{18}F-fluorodeoxyglucose in atherosclerotic mice. The noninvasive imaging techniques represent translational tools to assess the efficacy of phosphorylcholine-targeted therapy on coronary artery function and atherosclerosis in clinical studies. (J Am Coll Cardiol Basic Trans Science 2020;5:360–73) © 2020 The Authors. Published by Elsevier on behalf of the American College of Cardiology Foundation. This is an open access article under the CC BY-NC-ND license (http://creativecommons.org/licenses/by-nc-nd/4.0/).

ABBREVIATIONS AND ACRONYMS

^{18}F-FDG = ^{18}F-fluorodeoxyglucose

ANOVA = analysis of variance

ApoB = apolipoprotein-B

CFR = coronary flow reserve

HAEC = human aortic endothelial cell

Ig = immunoglobulin

ICAM = intracellular adhesion molecule

IL = interleukin

Lp(a) = lipoprotein(a)

LDLR = low-density lipoprotein receptor

NO = nitric oxide

OxLDL = oxidized low-density lipoprotein cholesterol

OxPLs = oxidized phospholipids

PC = phosphorylcholine

PC-mAb = human PC antibody

VCAM = vascular cell adhesion molecule

Oxidized phospholipids (OxPLs) mediate many atherogenic processes, including endothelial dysfunction, the accumulation of inflammatory cells into the vessel wall, and the uptake of oxidized low-density lipoprotein (OxLDL) cholesterol by macrophages, thereby promoting foam cell formation and atheroma growth (1–3).

Phosphorylcholine (PC) is the polar headgroup of the membrane phospholipid phosphatidylcholine. It is a pro-inflammatory epitope in OxPLs that is recognized as a danger-associated molecular pattern by the innate immune system (1). Human serum contains endogenous antibodies against oxidized epitopes, with the predominant antibody being immunoglobulin (Ig)-M antibody against PC (4–6). Low levels of IgM anti-PC are associated with an increased risk of atherosclerotic cardiovascular events in different patient populations (4,7–10). In subjects with elevated lipoprotein(a) [Lp(a)] and increased inflammatory activity in the arterial wall, activation of circulating monocytes by OxPLs can be inhibited by the IgM E06 antibody, the prototypic murine antibody against PC (11). Experimental studies have indicated that this antibody blocks the scavenger receptor-mediated uptake of OxLDL on macrophages in vitro (5), and that induction of the PC antibody formation by immunization (12,13) or direct infusion (14) is atheroprotective in mice. In transgenic mice, a single-chain variable fragment of E06 counteracts with OxPLs in vivo, attenuating inflammation and progression of atherosclerosis (15). Accordingly, the available evidence suggests that OxPLs that contain PC are a risk factor for atherosclerosis-related diseases and that a therapeutic antibody against PC may represent an

From the [a]Turku PET Centre, University of Turku, Turku, Finland; [b]Einthoven Laboratory for Experimental Vascular Medicine, Department of Surgery, Leiden University Medical Center, Leiden, the Netherlands; [c]Department of Experimental Vascular Medicine, Amsterdam Cardiovascular Sciences, Amsterdam University Medical Center (UMC), University of Amsterdam, Amsterdam, the Netherlands; [d]Research Center for Integrative Physiology and Pharmacology, Institute of Biomedicine, University of Turku, Turku, Finland; [e]Turku Center for Disease Modeling, University of Turku, Turku, Finland; [f]i3tex AB, Gothenburg, Sweden; [g]Department of Vascular Medicine, Academic Medical Center, Amsterdam University Medical Center (UMC), Amsterdam, the Netherlands; [h]A.I. Virtanen Institute for Molecular Sciences, University of Eastern Finland, Kuopio, Finland; [i]Department of Pathology and Forensic Medicine, University of Turku, Turku, Finland; [j]Athera Biotechnologies AB, Stockholm, Sweden; [k]Turku PET Centre, Turku University Hospital, Turku, Finland; [l]Heart Center, Turku University Hospital, Turku, Finland; and the [m]Institute of Clinical Medicine, Turku University Hospital, Turku, Finland. The study was conducted within the Finnish Centre of Excellence in Cardiovascular and Metabolic Diseases supported by the Academy of Finland, University of Turku, Turku University Hospital, Åbo Akademi University, the European Union's Seventh Framework Program Project CARDIMMUN (grant 601728), and the European Union Horizon 2020 research and innovation program REPROGRAM (grant agreement 667837). Ms. Ståhle and Drs. Roivainen, and Saraste were supported by the Finnish Foundation for Cardiovascular Research. Drs. Roivainen and Saraste were supported by the Sigrid Jusélius Foundation. Ms. Ståhle was supported by the Instrumentarium Science Foundation, the Finnish Cultural Foundation, and the Drug Research Doctoral Programme, University of Turku Graduate School, Turku, Finland. Dr. Kroon was supported by the Netherlands Organization for Scientific Research VENI (91619098). Drs. Pettersson and T. Abrahamsson have received consultancy fees from and hold shares in Athera Biotechnologies AB. Dr. Pettersson is named as co-inventor on patent applications regarding therapeutic antibodies to PC assigned to Athera Biotechnologies AB. Dr. Knuuti has been a consultant for GE Healthcare and AstraZeneca. Dr. Saraste has been a member of the Advisory Board for AstraZeneca; and has received speaker fees from AstraZeneca, Bayer, Novartis, and Abbott. All other authors have reported that they have no relationships relevant to the contents of this paper to disclose.

The authors attest they are in compliance with human studies committees and animal welfare regulations of the authors' institutions and Food and Drug Administration guidelines, including patient consent where appropriate. For more information, visit the *JACC: Basic to Translational Science* author instructions page.

Manuscript received January 30, 2019; revised manuscript received January 15, 2020, accepted January 15, 2020.

approach to improve coronary vascular function and attenuate atherosclerotic inflammation.

Positron emission tomography imaging with ^{18}F-fluorodeoxyglucose (^{18}F-FDG) is a noninvasive tool to measure inflammation in atherosclerotic lesions because ^{18}F-FDG accumulates in inflammatory cells (16,17). Coronary flow reserve (CFR) in response to vasodilator stress is an integrated measure of blood flow through both the epicardial coronary arteries and microvasculature (18). Impaired CFR is a strong predictor of cardiovascular mortality in patients with suspected coronary artery disease (19). Both ^{18}F-FDG uptake and CFR can serve as translational tools to assess the effects of anti-atherosclerotic therapy.

In the present study, we investigated whether a novel exogenous monoclonal IgG1 antibody against PC (designated X19-mu, with similar properties to the endogenous IgM E06 anti-PC) improves vascular function and reduces atherosclerotic inflammation in hypercholesterolemic low-density lipoprotein receptor deficient mice, expressing only apolipoprotein B100 (LDLR$^{-/-}$ApoB$^{100/100}$). Vascular function was studied by measuring CFR in response to adenosine with Doppler ultrasound and endothelium-mediated vasodilatation in response to methacholine. Inflammation in aortic atherosclerotic lesions was determined by the uptake of ^{18}F-FDG and histological stainings of inflammatory markers. The effect of human PC antibody (PC-mAb) on human aortic endothelial cells (HAECs) stimulated with Lp(a) was studied in vitro.

METHODS

X19-mu AND HUMAN PC-mAb. The antigen-binding sequences of the X19-mu antibody were identified from a phage display library on the basis of their binding ability to PC and were converted to full IgG1 antibodies as part of the work that identified PC-mAb, a fully human monoclonal antibody against PC. This therapeutic, exogenous PC-mAb (Clone X19-A05, Athera Biotechnologies AB, Stockholm, Sweden) showed similar properties to the IgM E06 antibody in inhibiting OxLDL uptake in macrophages, binding to apoptotic cells, blocking OxLDL-induced release of monocyte chemoattractant protein 1 from monocytes, binding to inflammatory cells in human aortic atherosclerotic lesions, and preventing inflammation-driven vascular remodeling in mice (20,21). X19-mu (Athera Biotechnologies AB) differs from the fully human PC-mAb in that it has a murine Fc fraction to lower the risk of an immune reaction to the treatment, but it has identical antigen-binding sequences. The binding affinity to PC is similar between the fully human PC-mAb and the X19-mu antibody (Supplemental Figure 1).

ANIMALS AND INTERVENTIONS. The national Animal Experiment Board in Finland and the Regional State Administrative Agency for Southern Finland approved the studies (license ESAVI/2163/04.10.07/2015). They were carried out in compliance with European Union laws related to the conduct of animal experimentation. The animals were housed under standard conditions with a 12-h light–dark cycle with ad libitum access to water and food.

LDLR$^{-/-}$ApoB$^{100/100}$ mice (n = 45; strain #003000, The Jackson Laboratory, Bar Harbor, Maine) were fed a high-fat diet (0.2% total cholesterol, TD 88137, Harlan Teklad, Harlan Laboratories, Madison, Wisconsin) for 12 weeks, starting at the age of 8 weeks, to induce atherosclerosis. After 12 weeks on the high-fat diet, 34 mice were continued on a regular chow diet; after sex and sibling matching, they were randomized to receive intraperitoneal injections containing either 0.9% saline solution as a vehicle (n = 17) or 10 mg/kg X19-mu (n = 17), once a week, for 6 weeks. A separate group of mice (n = 11) was studied at week 0, after the 12-week high-fat diet.

CFR was assessed repeatedly before and after 6 week treatments in a randomly selected, prespecified subgroup of mice (n = 10/treatment) and also in a separate group of healthy C57BL/6 mice (n = 11; age: 6.5 months). Aortic histology and ^{18}F-FDG uptake were assessed at the end of the 6-week treatments, and also at week 0, in a separate group of mice. Endothelium-mediated vasodilatory response to methacholine was studied in a separate group of atherosclerotic mice after treatment with vehicle (n = 8) or X19-mu antibody (n = 7). For euthanasia in aortic histology and ^{18}F-FDG studies, mice were anesthetized with isoflurane (2% to 3% inhalation), and blood was collected by cardiac puncture followed by cervical dislocation.

BLOOD SAMPLES. For details of the measurement of blood glucose, lipids and X19-mu antibody levels, see the Supplemental Appendix.

HISTOLOGY AND IMMUNOFLUORESCENCE. The aortic root was fixed with 10% formalin, embedded in paraffin, and cut into serial 5 μm cross sections at the level of the coronary ostium. Sections were stained with Movat's pentachrome for measurement of the atherosclerotic lesion area and with Masson's trichrome (Sigma-Aldrich, St. Louis, Missouri) for quantification of lesion collagen content. Macrophages were detected by double immunofluorescence using Mac-3 antibody and either CCR2 antibody that

detected M1 polarized macrophages or CD206 antibody that detected M2 polarized macrophages. Macrophage apoptosis was studied by double immunofluorescence using Mac-3 and cleaved caspase-3 antibodies. Furthermore, vascular cell adhesion molecule (VCAM)-1, intracellular adhesion molecule (ICAM)-1, interleukin (IL)-1β, and monocyte chemoattractant protein 1 were detected by immunofluorescence. The presence of PC epitope in atherosclerotic lesions was detected by immunofluorescence using the fully human PC-mAb directly labeled with Cy5 and co-stained with the Mac-3 antibody and CD31 antibody that detected endothelial cells (Supplemental Table 1). For details, see the Supplemental Appendix. Control stainings with nonimmune IgGs are presented in Supplemental Figure 2.

CFR AND ENDOTHELIUM-MEDIATED VASODILATATION. A dedicated small animal Doppler ultrasound device (Vevo 2100, VisualSonics Inc., Toronto, Ontario, Canada) with a linear 22- to 55-MHz (MS550D) transducer was used to assess CFR as previously described (22,23). Mice were anesthetized with an intraperitoneal injection of midazolam (8 mg/kg; Hameln Pharmaceuticals GmbH, Hameln, Germany) and ketamine (60 mg/kg; Intervet International BV, Boxmeer, the Netherlands). A tail vein was cannulated, and body temperature was maintained with a heating pad. Blood flow in the middle left coronary artery was localized under color Doppler mapping using modified long-axis views, and the flow velocity spectrum was recorded by pulsed-wave Doppler, both at rest and during infusion (maximum of 2 min) of adenosine (140 μg/kg/min; Life Medical Sweden AB, Stocksund, Sweden). Anesthesia was reversed with a subcutaneous injection of flumazenil (0.5 mg/kg; Hameln Pharmaceuticals GmbH). CFR was calculated as the ratio of the mean diastolic flow velocity during maximal adenosine-induced hyperemia to that during rest. The mice were allowed to recover for a minimum of 72 h between ultrasound and ^{18}F-FDG studies.

Endothelium-mediated vasodilatation was studied by measuring arterial blood pressure response to intravenous injection of methacholine in apolipoprotein E deficient (ApoE$^{-/-}$) mice (Supplemental Appendix).

STIMULATION OF HAECs WITH DONOR-DERIVED LP(a). To study the effect of PC-mAb on endothelial nitric oxide (NO) production and inflammatory responses, HAECs were stimulated with 1 mg/ml of Lp(a) for 24 h in the presence of fully human PC-mAb or a non-specific IgG. Thereafter, cells were processed for gene expression measurements of *VCAM1*, *ICAM1*, *IL6*, and *IL8*, as well as protein measurements of IL-6 and IL-8, or lysed for measurement of intracellular nitrate reflecting NO production (Supplemental Appendix).

^{18}F-FDG UPTAKE. The mice were fasted for 4 h, anesthetized with isoflurane, and then intravenously injected with ^{18}F-FDG (11 ± 0.38 MBq) via the tail vein. At 90 min post-injection, the thoracic aorta from the sinotubular junction to the level of the diaphragm was excised and rinsed with saline. The aorta was frozen in cooled isopentane and cut into sequential longitudinal cryosections of 20 and 8 μm, which provided sections throughout the region on a single slide (n = 6 to 8 intervals per aorta). Digital autoradiography was performed using the previously described method (24,25). Cryosections were apposed to an imaging plate (Fuji Imaging Plate BAS-TR2025, Fuji Photo Film Co., Ltd., Tokyo, Japan) for 4 h and then scanned with a Fuji Analyser BAS-5000 (internal resolution of 25 μm, Fuji). Then, sections were stained with hematoxylin and eosin (20 μm) or immunohistochemically with Mac-3 antibody (8 μm), scanned with a slide scanner, and co-registered with autoradiographs. ^{18}F-FDG accumulation was measured as photo-stimulated luminescence per square millimeter in regions of interest placed on the atherosclerotic lesions (n = 22/mouse) and vessel walls without lesions (n = 16/mouse), using Tina 2.1 software (Raytest Isotopenmessgeräte, GmbH, Straubenhardt, Germany). To assess the treatment effects, the average ^{18}F-FDG uptake within all atherosclerotic lesions in 20-μm sections was calculated and divided by the average uptake in lesion-free vessel walls (expressed as lesion-to-wall ratio) in each mouse. To assess the effects of treatment on ^{18}F-FDG uptake in atherosclerotic lesions with different macrophage densities, percentage of Mac-3-positive staining within the lesions was measured with Image J software and compared with the ^{18}F-FDG uptake (lesion-to-wall ratio) in the same lesions in 8 μm sections (n = 7 randomly chosen mice/treatment; 8 lesions/mouse) as previously described (25). Measurement of ^{18}F-FDG uptake in other organs is described in the Supplemental Appendix.

STATISTICAL ANALYSIS. Results are presented as individual data points with mean ± SD, unless otherwise indicated. Data were analyzed using SPSS Statistics software 22 (IBM, Armonk, New York). Normality was examined by a Shapiro-Wilk test, and equality of variances was tested with Levene's test. Multiple comparisons were made by 1-way analysis of variance (ANOVA) followed by Dunnett's post hoc test for the week 0 group. Student's *t*-test for unpaired or paired data was used for comparisons between intervention groups. Fisher's exact test was used to evaluate

histological scores. Mann-Whitney U test was applied for in vitro data analysis. Analysis of covariance was used for repeated measurements, which adjusted each subject's follow-up measurement according to their baseline measurement, and was used to compare CFR values. There were no differences between female and male mice, except in the ^{18}F-FDG study, in which the level of ^{18}F-FDG uptake was higher in females. Sex by group interaction was examined and although it was not statistically significant, group and sex were included as fixed factors in the model. Two-way ANOVA was used to compare ^{18}F-FDG uptake in lesions divided into tertiles according to macrophage density. Macrophage density and treatment were included as fixed factors in the model (no interaction between macrophage density and treatment was observed). A p value of <0.05 was considered statistically significant. Assuming an average CFR of 2.5 ± 0.3 (23) and ^{18}F-FDG uptake of 1.8 ± 0.25 (25), sample sizes of 10 and 14 were calculated to be sufficient to detect a difference of 15% with 80% power and a type I error of 0.05, respectively.

RESULTS

Treatment with X19-mu was well tolerated, with the antibody remaining present in the blood until the end of the intervention; the average plasma X19-mu concentration 5 to 7 days after the last injection was 14 ± 9.8 μg/ml. One mouse was excluded due to a failure in the dosing of X19-mu (no detectable levels of X19-mu in plasma), and 1 mouse due to failure in dosing of ^{18}F-FDG. Thus, the final study group consisted of 16 mice in the vehicle group and 16 mice in the X19-mu group.

As shown in Table 1, the body weights and fasting blood glucose levels were comparable between the vehicle- and X19-mu–treated groups. Compared with the mice studied at week 0, plasma levels of cholesterol, LDL, and high-density lipoprotein were lower ($p \leq 0.001$) after 6 weeks on normal mouse chow in both the vehicle and X19-mu groups, with the X19-mu treatment not showing any incremental effect on lipids in comparison with vehicle.

LESION HISTOLOGY. All LDLR$^{-/-}$ApoB$^{100/100}$ mice showed prominent macrophage-rich atherosclerotic lesions in the aortic root (Figures 1 and 2). Compared with mice studied at week 0, the absolute lesion area in the aortic root was larger after the 6-week treatment in both the vehicle- (0.32 ± 0.23 mm^2 vs. 0.68 ± 0.28 mm^2; p = 0.004) and X19-mu–treated (0.32 ± 0.23 mm^2 vs. 0.62 ± 0.28 mm^2; p = 0.017) mice. However, the lesion areas were similar after treatment with either vehicle or X19-mu (p = 0.57).

TABLE 1 Characteristics of LDLR$^{-/-}$ApoB$^{100/100}$ Mice at the Time of Randomization (Week 0) and After 6-Week Treatment With Vehicle or X19-mu Antibody

	Week 0	Vehicle	X19-mu
Animals (f/m)	11 (5/6)	16 (8/8)	16 (8/8)
Body weight (g)	28 ± 5.1	30 ± 6.0	30 ± 7.7
Blood glucose (mmol/l)	11 ± 2.7	10 ± 2.6	10 ± 2.3
Total cholesterol (mmol/l)	29 ± 6.7	8.8 ± 1.6*	9.0 ± 1.8*
LDL	26 ± 6.3	6.8 ± 1.3*	7.0 ± 1.6*
HDL	5.9 ± 2.2	2.6 ± 0.67*	2.8 ± 0.58*
Triglycerides (mmol/l)	1.7 ± 0.52	1.5 ± 0.45	1.5 ± 0.53

Values are mean ± SD. One-way analysis of variance with Dunnett's post-hoc test. *p < 0.01 vs. week 0.

ApoB = apolipoprotein-B; F = female; HDL = high-density lipoprotein; LDL = low-density lipoprotein; LDLR = low-density lipoprotein receptor; M = male.

At week 0, the intimal area positive for Mac-3 staining was 25 ± 8.2%. In comparison with this initial value, the intimal area positive for Mac-3 did not differ after the 6-week treatment with vehicle (19 ± 8.7%; p = 0.19) or X19-mu (19 ± 10%; p = 0.21). X19-mu treatment had no effect in comparison with vehicle (p = 0.93) (Figure 1G). The expression of the M1 macrophage marker CCR2 after vehicle treatment was comparable to that in the X19-mu–treated group (44 ± 13% vs. 43 ± 13% of the Mac-3 positive area; p = 0.87) (Figure 1H), as was the expression of the M2 macrophage marker CD206 (48 ± 26% vs. 60 ± 24% of the Mac-3 positive area; p = 0.23) (Figure 1H), which resulted in a comparable ratio of M2 and M1 macrophages (1.4 ± 1.1 vs. 1.7 ± 1.3; p = 0.55). At week 0, the percentages of M1 and M2 macrophages were 41 ± 9.2% and 50 ± 13%, respectively. These values were similar after 6-week treatment with either vehicle (p = 0.84 and p = 0.96, respectively) or X19-mu (p = 0.91 and p = 0.60, respectively).

The extent of lesion endothelium positive for VCAM-1 or ICAM-1 did not show significant differences after treatment with vehicle or X19-mu (median [25% and 75% percentiles] score: 2.5 [2.0 and 3.0] vs. 2.0 [2.0 and 3.0], p = 0.65 and 2.5 [2.0 and 3.0] vs. 2.0 [1.0 and 2.0]; p = 0.32) (Figures 2A and 2B, respectively). Compared with vehicle, treatment with X19-mu reduced the intimal area positive for IL-1β (24 ± 1.0% vs. 21 ± 0.83%; p = 0.044) (Figure 2C) but not for monocyte chemoattractant protein 1 (10 ± 1.0% vs. 10 ± 0.60%; p = 0.82) (Figure 2D). The number of macrophages containing cleaved caspase-3 was similar after treatment with vehicle or X19-mu (220 ± 65 cells/mm^2 vs. 230 ± 72 cells/mm^2; p = 0.61) (Figure 2E). The lesion collagen content was similar after treatment with vehicle or X19-mu (39 ± 5.6% vs. 40 ± 7.9%; p = 0.68) (Figure 2F).

FIGURE 1 **Macrophage Proportion or Phenotype in Atherosclerotic Lesions Is Not Affected by X19-mu Treatment**

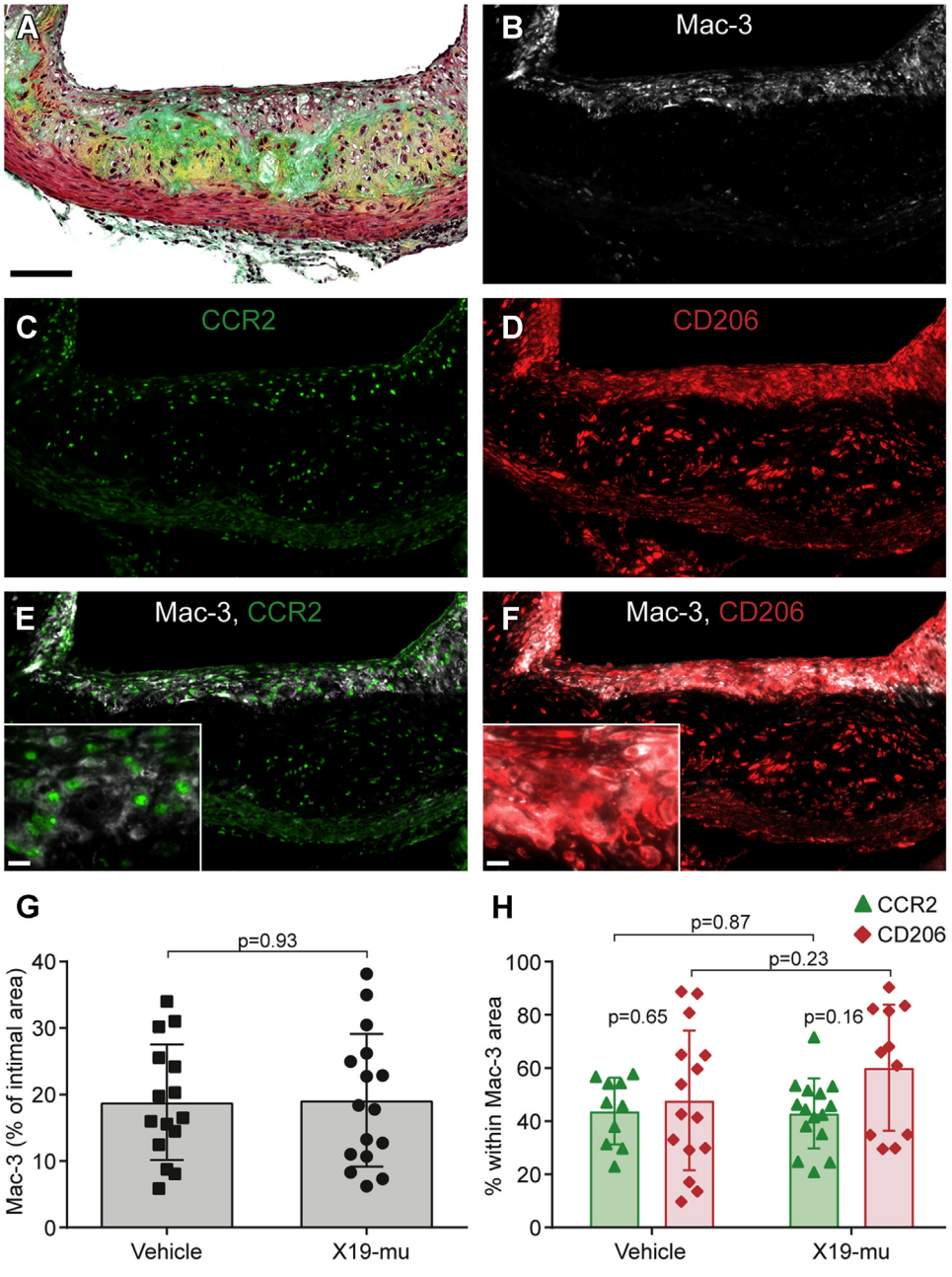

An atherosclerotic lesion from serial sections of the aortic root stained with **(A)** Movat's pentachrome, **(B)** antibodies against Mac-3 in macrophages, **(C)** CCR2 in M1 polarized macrophages, and **(D)** CD206 in M2 polarized macrophages, as well as double immunofluorescence stainings with **(E)** Mac-3 and CCR2, or **(F)** Mac-3 and CD206. The percentage of intimal area **(G)** stained with Mac-3 and the **(H)** proportions of CCR2- and CD206-positive macrophages within the Mac-3 area shown as individual data points with mean ± SD. Student's *t*-test for unpaired and paired (CCR2 vs. CD206) measurements; n = 10 to 16/staining/group. **Scale bar** = 100 μm (10 μm in inserts in **E and F**).

FIGURE 2 The Effect of X19-mu Treatment on Lesion Histology in Aortic Root Sections

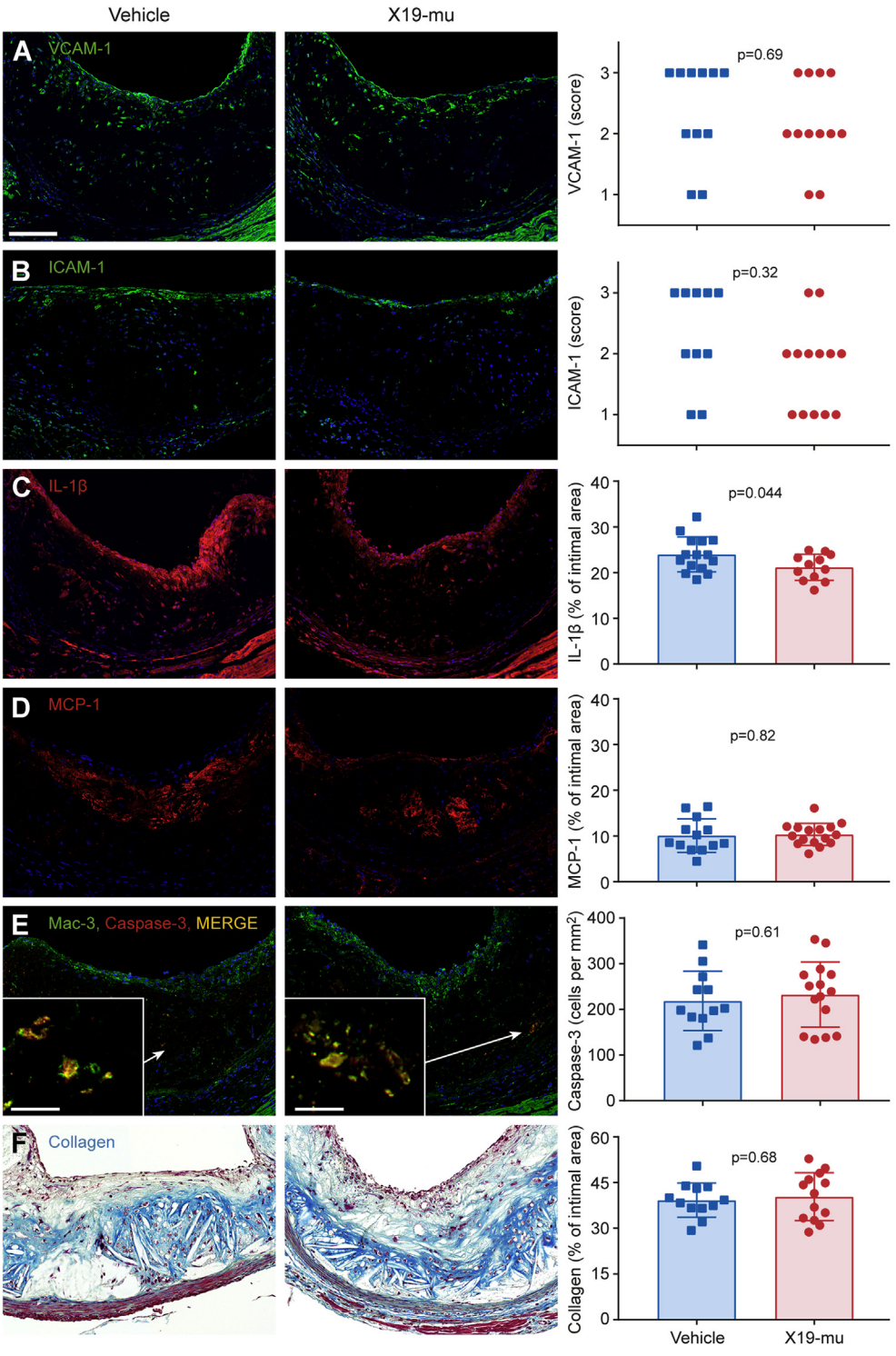

(A) Atherosclerotic lesions in the aortic root stained with vascular cell adhesion molecule (VCAM)-1 **(green)**, **(B)** intracellular cell adhesion molecule (ICAM)-1 **(green)**, **(C)** interleukin (IL)-1β **(red)**, **(D)** monocyte chemoattractant protein (MCP)-1 **(red)**, as well as **(E)** Mac-3 and cleaved caspase-3 **(yellow)**. All sections are counterstained with 4',6-diamino-2-phenylindole (**blue**, nuclei). **(F)** Lesion collagen content is quantified from Masson's trichrome stainings **(blue)**. Quantitative results are shown as individual data points in addition to mean ± SD in histograms; Fisher's exact test for histological scores **(A and B)**, and Student's *t*-test for unpaired measurements **(C to F)**; n = 10 to 16/staining/group. **Scale bar** = 100 μm (10 μm in inserts in **E**).

FIGURE 3 **PC Epitope Is Present in Endothelial Cells and Macrophages in Atherosclerotic Lesions**

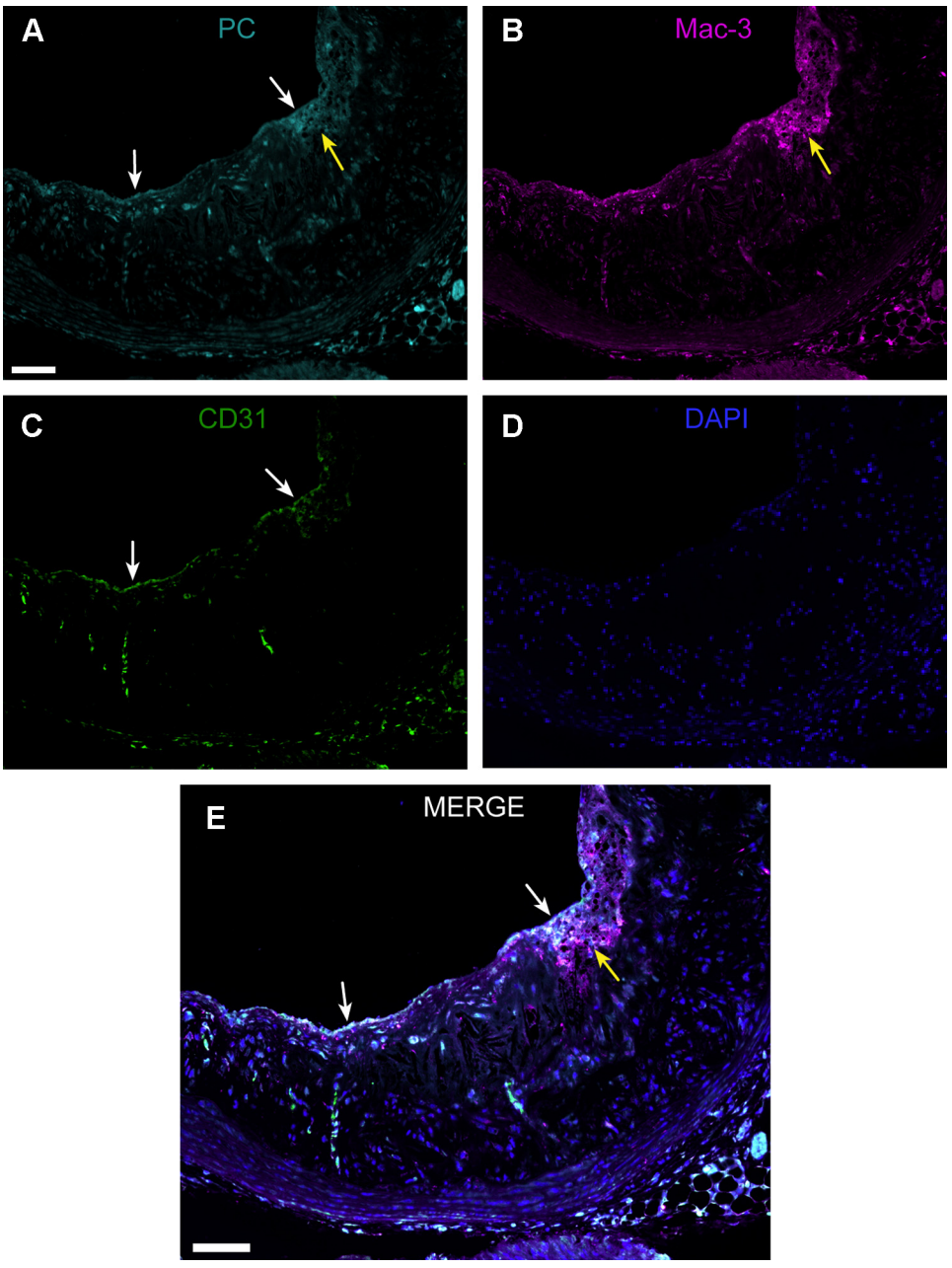

Representative section of the **(A)** aortic root showing immunofluorescence staining with phosphorylcholine (PC) antibody (PC-mAb), **(B)** Mac-3 antibody (macrophages), **(C)** CD31 antibody (endothelial cells), and **(D)** 4',6-diamino-2-phenylindole (DAPI, nuclei). **White arrows** indicate endothelial cells and **yellow arrows** macrophage-rich area. **(E)** PC-positive staining co-localizes with endothelial cells covering the lesion and macrophages (**white color** in merge). **Scale bar** = 75 μm. Abbreviation as in Figure 2.

Triple immunofluorescence staining demonstrated PC-positive staining that co-localized with Mac-3-positive macrophages within atherosclerotic lesions and CD31-positive endothelial cells covering the lesions (Figure 3).

X19-mu TREATMENT PRESERVED CFR AND ENDOTHELIUM-MEDIATED VASODILATATION. The CFR was measured as the ratio of coronary flow velocity in the left coronary artery during adenosine stress and rest by Doppler ultrasound (Figure 3A).

FIGURE 4 X19-mu Treatment Preserves CFR

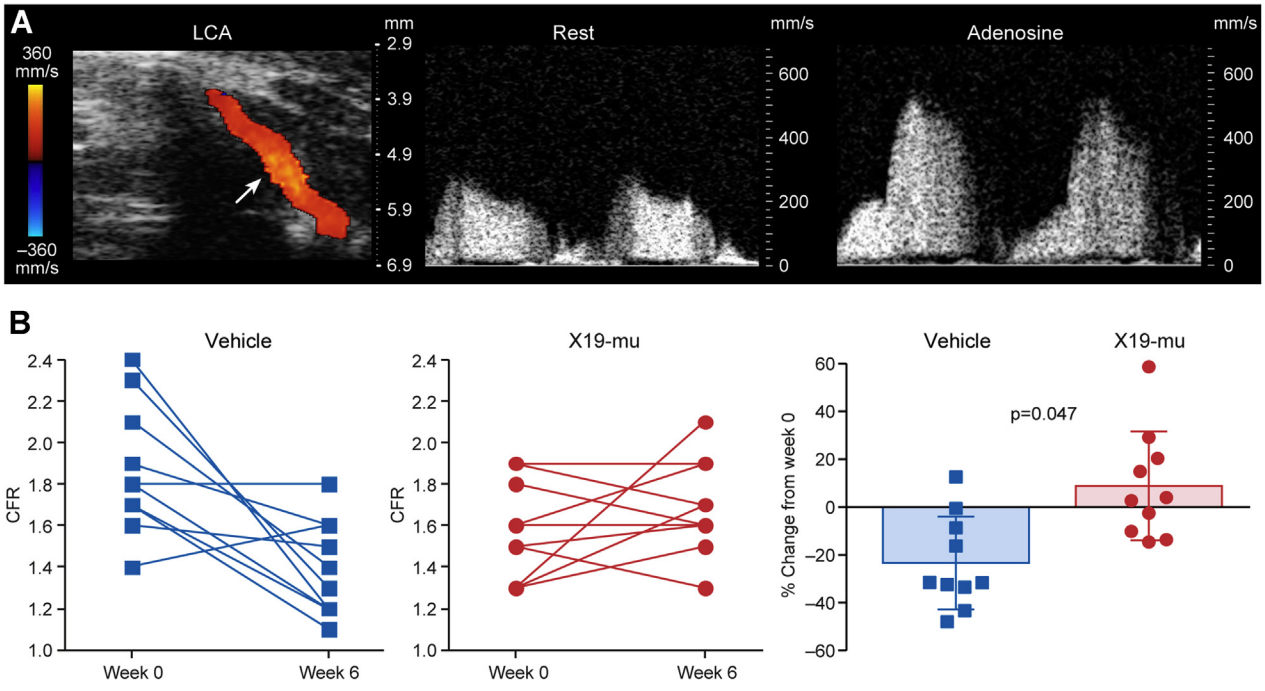

(A) Blood flow in the left coronary artery (LCA) localized under color Doppler mapping **(arrow)** and the blood flow velocity profiles recorded by pulsed-wave Doppler at rest and during adenosine infusion. Coronary flow reserve (CFR) in individual mice at week 0 and after a 6-week treatment with vehicle or X19-mu. **(B)** Compared with vehicle, the CFR adjusted by the week 0 measurement was improved ($p = 0.047$) after a 6-week treatment with X19-mu. Results are expressed as individual data points with mean ± SD in the histogram; analysis for covariance for repeated measurements; $n = 10$/group.

Analysis of covariance for repeated measurements showed that the treatment with X19-mu was associated with a 33% improvement in CFR ($p = 0.047$) compared with vehicle during the 6-week study period (Figure 4B). Compared with week 0, CFR was 24 ± 20% lower after the 6-week treatment with vehicle (1.9 ± 0.29 vs. 1.4 ± 0.23; $p = 0.006$), whereas there was a trend toward a higher (9.0 ± 23%) CFR after treatment with X19-mu (1.6 ± 0.24 vs. 1.7 ± 0.24; $p = 0.32$) (Figure 4B). In healthy age-matched C57BL/6 mice, CFR was higher (2.1 ± 0.39) than in atherosclerotic mice after either vehicle or X19-mu treatment ($p < 0.001$ and $p = 0.003$, respectively). The absolute flow velocities are shown in the Supplemental Table 2. In a separate group of atherosclerotic ApoE$^{-/-}$ mice, methacholine injection induced a transient reduction in arterial blood pressure (vasodilatory response) in X19-mu–treated mice, but not in the vehicle group (Supplemental Appendix, Supplemental Figure 3).

PC-mAb TREATMENT PRESERVED NO PRODUCTION IN HAECs. To investigate the mechanistic effects of human PC-mAb treatment on endothelium, HAECs were stimulated with isolated Lp(a), the main carrier of PC/OxPLs (11). In HAECs, intracellular nitrate concentration was decreased after 24-h stimulation with Lp(a) in the presence of a nonspecific IgG (median [25% and 75% percentiles]: 144 [143 and 150] pmol/$\times 10^6$ cells vs. 118 [117 and 123] pmol/$\times 10^6$ cells; $p = 0.049$) but was preserved in the presence of PC-mAb (135 [133 and 172] pmol/$\times 10^6$ cells, $p = 0.049$ vs. nonspecific IgG) (Figure 5A). *VCAM1*, *ICAM1*, and *IL8* gene-expression tended to be lower in the presence of PC-mAb than nonspecific IgG but were not statistically significant. *IL6* gene-expression as well as IL-6 and IL-8 protein levels were similar in the presence of PC-mAb and nonspecific IgG antibodies (Figure 5B).

X19-mu TREATMENT REDUCED ^{18}F-FDG UPTAKE IN ATHEROSCLEROTIC LESIONS. Autoradiography showed focal uptake of ^{18}F-FDG in macrophage-rich atherosclerotic lesions within the aorta (Figures 6A to 6C). Compared with vehicle-treated mice and adjusted by sex, the average uptake of ^{18}F-FDG in atherosclerotic lesions normalized to activity in the lesion-free vessel wall (lesion-to-wall ratio) was significantly lower after the 6-week treatment with X19-mu (1.7 ± 0.24 vs. 1.5 ± 0.17, $p = 0.002$)

FIGURE 5 PC-mAb Treatment Preserves NO Production in Human Aortic Endothelial Cells

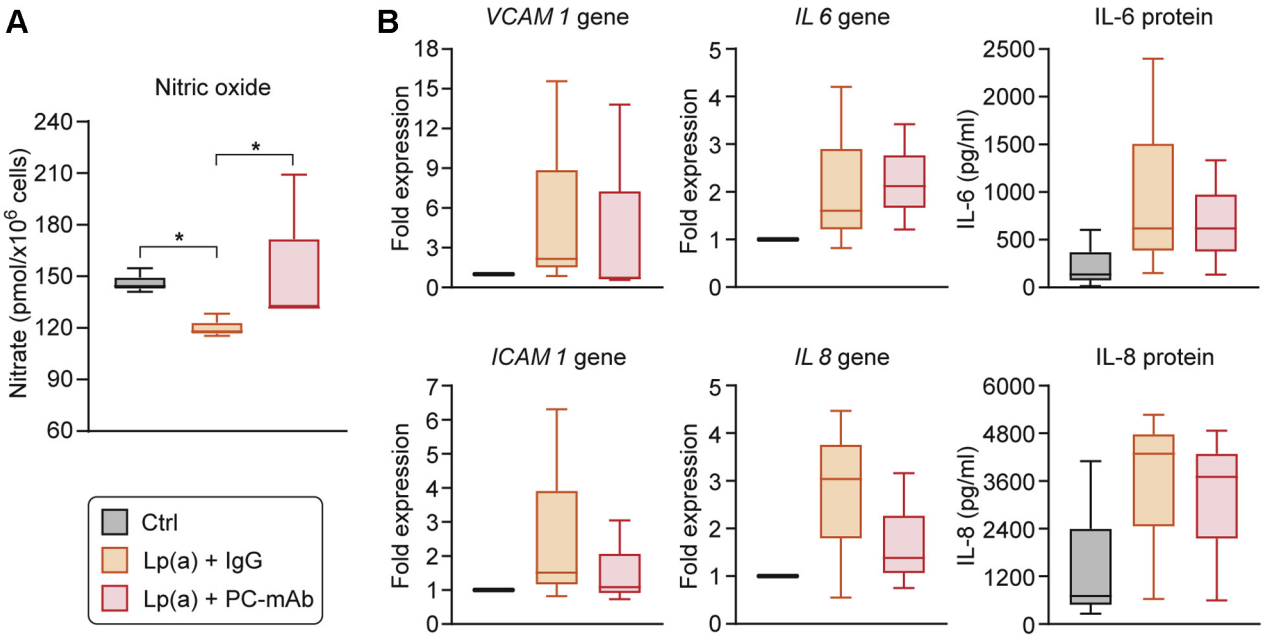

(A) Intracellular nitrate reflecting nitric oxide (NO) production was significantly decreased after 24-h stimulation with lipoprotein(a) [Lp(a)] in the presence of a nonspecific immunoglobulin-G (IgG) but preserved in the presence of PC-mAb. **(B)** The pro-inflammatory mediators, *VCAM1*, *ICAM1*, and *IL8* gene-expression tended to be lower in the presence of PC-mAb than the nonspecific IgG antibody, but it was not statistically significant (**B**). Results are expressed as median with 25th and 75th percentiles for 3 independent experiments; Mann-Whitney U test; *p < 0.05. Ctrl = control; other abbreviations as in Figures 2 and 3.

(Figure 6D). If analyzed separately, ^{18}F-FDG uptake was reduced after X19-mu treatment in both females ($p = 0.023$) and males ($p = 0.034$) compared with vehicle (Supplemental Figure 4). In comparison to the ^{18}F-FDG uptake at week 0 in the mice fed a high-fat diet (2.3 ± 0.24), the lesion-to-wall ratios were lower after the 6-week treatment on normal mouse chow in both the vehicle- ($p < 0.001$) and X19-mu–treated ($p < 0.001$) groups.

The uptake of ^{18}F-FDG was further compared in lesions with low (average 22%), intermediate (29%), or high (35%) density of macrophages. The^{18}F-FDG uptake was gradually increased in these lesions and was highest in lesions with high density of macrophages ($p = 0.039$). However, X19-mu treatment reduced ^{18}F-FDG uptake in lesions with low, intermediate. and high macrophage density compared with vehicle ($p < 0.001$) (Figure 6E). The ^{18}F-FDG uptake in other tissues is presented in Supplemental Table 3.

DISCUSSION

Our results revealed that 6-week treatment with an exogenous antibody targeting PC epitope on OxPLs preserved CFR and reduced ^{18}F-FDG uptake in atherosclerotic lesions in mice. These results provided evidence that the therapeutic antibody against PC had beneficial effects on coronary vascular function and inflammatory activity in the arterial wall in atherosclerosis. Furthermore, our results indicated that CFR and ^{18}F-FDG PET could be used as possible surrogate markers for the efficacy of PC antibody therapy in future clinical studies.

Endothelial cell injury at early stages of atherosclerosis may lead to exposure of antigens, including OxPLs, that are normally hidden, eliciting an immune response and secretion of various disease-modifying antibodies (4,26). Previous studies indicated that OxPLs cause endothelial dysfunction with impairment of NO-mediated vasodilatation in arterial preparations (3,27). In patients with stable coronary artery disease, levels of the PC epitope in LDL particles were shown to be significantly related to the severity of endothelial dysfunction after lipid-lowering therapy (2). Furthermore, a negative correlation between OxLDL levels and CFR, an integrated measure of coronary reactivity (18), was found in young individuals with hypercholesterolemia (28). Our results extended the previous findings by

FIGURE 6 X19-mu Treatment Reduces ^{18}F-FDG Uptake in Atherosclerotic Lesions

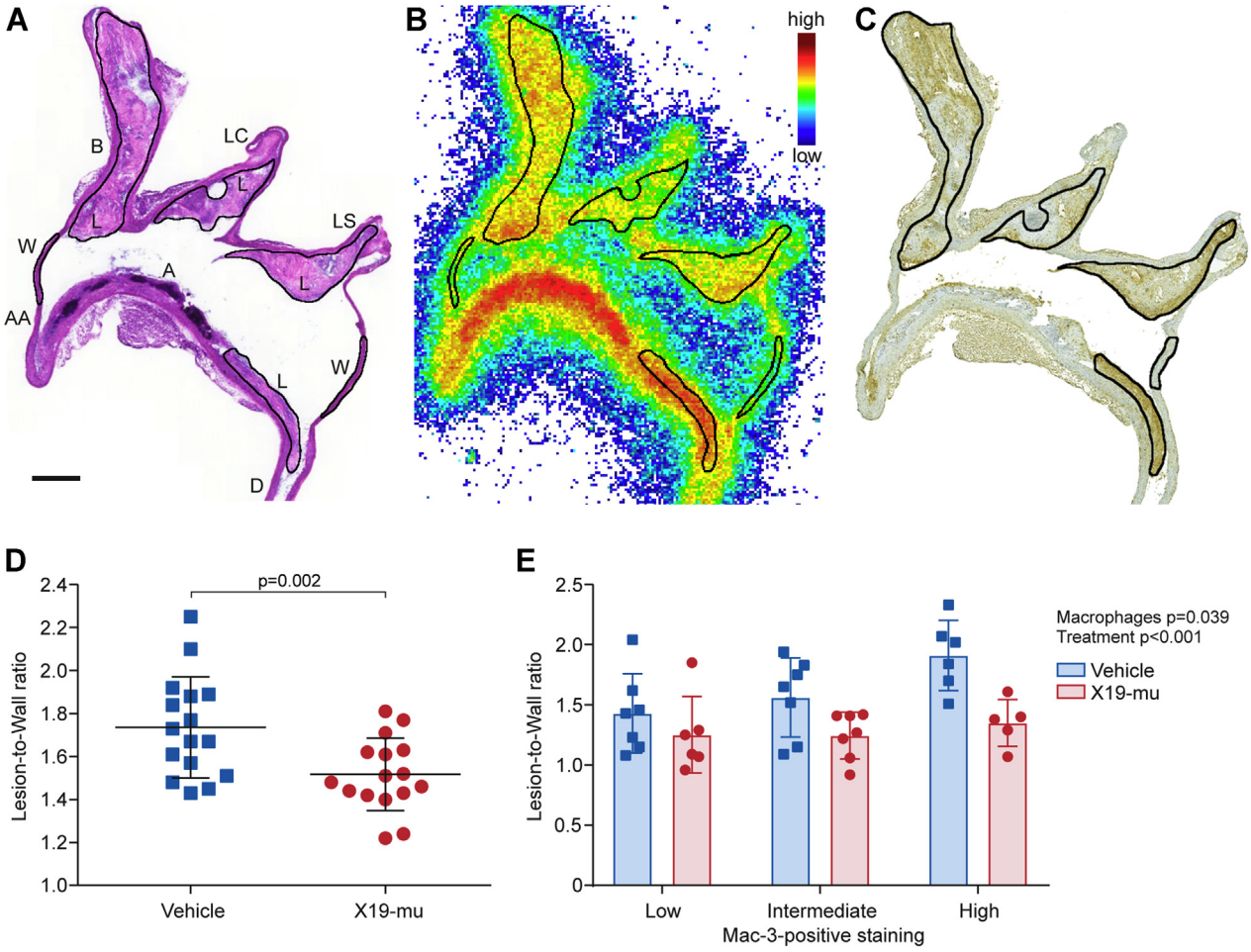

(A) A hematoxylin and eosin–stained longitudinal aortic cryosection, **(B)** corresponding autoradiograph, and **(C)** macrophage (Mac-3) staining. **Black lines** represent contours of the regions of interest defined in the atherosclerotic lesions and vessel wall without lesions. **(D)** The graph shows average 18-F-fluorodeoxyglucose (^{18}F-FDG) uptake in atherosclerotic lesions (normalized by the activity of vessel wall; lesion-to-wall ratio), which was lower after a 6-week treatment with X19-mu than with vehicle. (n = 16 mice/group; mean ± SD; sex-adjusted model). **(E)** The subanalysis showed that X19-mu treatment reduced ^{18}F-FDG uptake (lesion-to-wall ratios) in lesions with low, intermediate, and high macrophage density compared with vehicle. (n = 5 to 7 mice/group in each subcategory; mean ± SD; 2-way analysis for variance for the main effects of macrophage density and treatment). **Scale bar** = 0.5 mm. A = arch; AA = ascending aorta; B = brachiocephalic artery; D = descending thoracic aorta; L = lesion; LC = left common carotid artery; LS = left subclavian artery; W = wall.

providing evidence that a therapeutic antibody against PC preserved CFR in vivo in response to adenosine in hypercholesterolemic mice that had impaired CFR, despite the absence of obstructive coronary artery disease (22).

In HAECs stimulated with Lp(a), the main carrier of PC/OxPLs in the human plasma (11), the PC-mAb preserved NO production compared with that of a nonspecific IgG. In vivo, the methacholine provocation test further demonstrated enhanced vasodilatory response after X19-mu treatment. We previously showed that blood pressure response to methacholine could be blocked by pre-treatment with 50 mg/kg of the NO synthase inhibitor, L-Nitro-Arginine-Methyl Ester, which indicated NO- and endothelium-mediated mechanisms (29). These results indicated that the beneficial effects of X19-mu on CFR were at least partly mediated via direct effects on endothelial cell NO metabolism. In line with that, our immunofluorescence stainings demonstrated PC-positive staining in the aortic root sections co-localizing with endothelial cells and macrophages. Alternatively,

improved vasodilatory response might be a result of an anti-inflammatory effect of X19-mu, because inflammation is well known to hamper endothelium-mediated vascular control (4). Although it showed a modest effect, PC-mAb treatment did not lead to a statistically significant difference in the expression of pro-inflammatory mediators.

Uptake of ^{18}F-FDG in atherosclerotic lesions correlates with the quantity of inflammatory macrophages with high glucose consumption (16). Regardless of reflecting macrophage polarization (30), it has been shown that OxLDL stimulates macrophage ^{18}F-FDG uptake (31), and that ^{18}F-FDG uptake is particularly high in the early phase of foam cell formation (32). Recently, increased ^{18}F-FDG uptake in the arterial wall was found in patients with elevated Lp(a). Ex vivo experiments showed that the arterial inflammation was due to the OxPLs bound to Lp(a), because the E06 antibody prevented the pro-inflammatory effects of Lp(a) (11). The present study demonstrated that administration of a therapeutic antibody against PC reduced ^{18}F-FDG uptake in atherosclerotic lesions with different macrophage densities in vivo, which indicated reduced metabolic activity and possibly reduced anti-inflammatory effects in atherosclerosis. In line with this and a previous study (15), IL-1β was reduced in the lesions after X19-mu treatment. However, no changes in macrophage apoptosis was observed. The absolute amount of reduction in ^{18}F-FDG uptake (13%) was in line with the degree of reduction in arterial ^{18}F-FDG uptake seen in clinical studies that used cholesterol lowering intervention with atorvastatin (5% to 15%) (16,17). Previously, treatment with human recombinant IgG1 antibody against a malondialdehyde-modified ApoB100 peptide, another immunogenic epitope on OxLDL, did not reduce arterial ^{18}F-FDG uptake in hypercholesterolemic minipigs (33) or patients with stable inflammatory vascular lesions (34). These differences can be explained by differences in PC (phospholipid) and malondialdehyde (protein) epitopes, with the former being specifically associated with OxPLs (11) that are more prevalent in advanced, inflamed lesions (35).

Despite reduced ^{18}F-FDG uptake, we did not find a reduction in overall lesion macrophage quantity, the proportions of M1/M2 polarized macrophages, the lesion collagen content, or the atherosclerosis burden. Based on our previous validation study (24), mice that showed extensive pre-existing atherosclerosis at the beginning of therapy were studied, and therefore, it was unlikely that major plaque regression or changes in plaque cellular composition would have occurred within short-term treatment. Previous studies indicated that a metabolic marker such as ^{18}F-FDG uptake was sensitive to changes caused by short-term interventions, despite changes in plaque burden, and aortic ^{18}F-FDG signal provided an independent predictor of future cardiovascular events (16,17). There are also regional differences in the driving forces of atherogenesis in mice. Although histology was analyzed in the aortic root, ^{18}F-FDG uptake was measured throughout the thoracic aorta in different regions (36). Aortic root is the most common and validated region for atherosclerosis quantification, but also contains the most advanced lesions (36). Finally, macrophages in the lesions were mainly of the reparative M2 type before therapy, and there was a high variation in the proportions of M1/M2 polarized macrophages between mice; therefore, we could not exclude small effects of PC antibody treatment on macrophage phenotype.

STUDY LIMITATIONS. We did not assess ^{18}F-FDG uptake repeatedly in the same mice because high radiation exposure related to the high-resolution angiography might have influenced health of study animals, and the partial volume effects could have impaired the accuracy of quantification of the signal in the small atherosclerotic lesions in vivo (37). Although the LDLR$^{-/-}$ApoB$^{100/100}$ mouse is a widely used model of atherosclerosis, with a lipid profile that closely resembles human familial hypercholesterolemia, the findings could not be directly extrapolated to humans. Because of the high variation in CFR values observed in mice in general (from 1.2 to >2.2) (23,38) and in individual mice in our study, larger studies are needed to confirm the magnitude of the treatment effect on coronary vascular function. The high-fat diet was discontinued at the time of intervention, to prevent the toxic effects of high cholesterol and to mimic a clinical situation, where any therapy would be prescribed on top of cholesterol-lowering intervention. Chimeric mouse-human antibody was used in this study, because of the possible risk of formation of neutralizing antibodies with a fully human antibody in mice. Saline was used as a control treatment in the in vivo study because of challenges in the production of a corresponding mouse-human chimeric IgG1 not binding to PC, as well as to reduce the risk of interference of nonspecific IgG with the naturally occurring antibody responses (26).

CONCLUSIONS

Six weeks of treatment with X19-mu, a chimeric IgG1 antibody against PC on OxPLs, preserved coronary

artery function and attenuated uptake of ^{18}F-FDG in atherosclerotic lesions in mice. The present findings provide evidence that X19-mu exerts therapeutic actions on endothelial cell function and inflammatory processes in the vessel wall, despite changes in lesion burden or cholesterol levels. Our results suggest that noninvasive imaging techniques, CFR and ^{18}F-FDG PET measures, represent translational tools to assess the effects of PC-targeted therapy on vascular function and atherosclerosis in clinical studies.

ACKNOWLEDGMENTS The authors thank Jenni Virta, Aake Honkaniemi, Erica Nyman, Marja-Riitta Kajaala, Liisa Lempiäinen, Erna Peters, Laura Parma, Miranda Versloot, Eliisa Löyttyniemi, Timo Kattelus, and Cell Imaging and Cytometry Core at Turku Bioscience Centre for technical assistance.

ADDRESS FOR CORRESPONDENCE: Dr. Antti Saraste, Turku PET Centre, Turku University Hospital, Kiinamyllynkatu 4-8, FI-20520 Turku, Finland. E-mail: antti.saraste@utu.fi.

PERSPECTIVES

COMPETENCY IN MEDICAL KNOWLEDGE: Proinflammatory OxPLs that contain PC are a risk factor for cardiovascular disease. The present study demonstrated that treatment with a therapeutic monoclonal IgG1 antibody against PC on OxPLs affected NO metabolism in endothelial cells, preserved CFR, and attenuated atherosclerotic inflammation as determined by the uptake of ^{18}F-FDG in atherosclerotic mice. The results provided proof-of-concept that a therapeutic antibody targeting PC might represent an approach to inhibit the atherogenic impact of OxPLs.

TRANSLATIONAL OUTLOOK: The noninvasive imaging techniques represent translational tools to assess the effects of PC-targeted therapy on coronary artery function and atherosclerosis and appear to be possible surrogate markers for the efficacy of this therapy in clinical studies.

REFERENCES

1. Miller YI, Choi SH, Wiesner P, et al. Oxidation-specific epitopes are danger-associated molecular patterns recognized by pattern recognition receptors of innate immunity. Circ Res 2011;108:235–48.

2. Penny WF, Ben-Yehuda O, Kuroe K, et al. Improvement of coronary artery endothelial dysfunction with lipid-lowering therapy: heterogeneity of segmental response and correlation with plasma-oxidized low density lipoprotein. J Am Coll Cardiol 2001;37:766–74.

3. Rikitake Y, Hirata K, Kawashima S, Inoue N. Inhibition of endothelium-dependent arterial relaxation by oxidized phosphatidylcholine. Atherosclerosis 2000;152:79–87.

4. Iseme RA, Mcevoy M, Kelly B, et al. A role for autoantibodies in atherogenesis. Cardiovasc Res 2017;113:1102–12.

5. Shaw PX, Hörkkö S, Chang MK, et al. Natural antibodies with the T15 idiotype may act in atherosclerosis, apoptotic clearance, and protective immunity. J Clin Invest 2000;105:1731–40.

6. Fiskesund R, Su J, Bulatovic I, Vikström M, de Faire U, Frostegård J. IgM phosphorylcholine antibodies inhibit cell death and constitute a strong protection marker for atherosclerosis development, particularly in combination with other autoantibodies against modified LDL. Results Immunol 2012;2:13–8.

7. Gigante B, Leander K, Vikström M, et al. Low levels of IgM antibodies against phosphorylcholine are associated with fast carotid intima media thickness progression and cardiovascular risk in men. Atherosclerosis 2014;236:394–9.

8. Caidahl K, Hartford M, Karlsson T, et al. IgM-phosphorylcholine autoantibodies and outcome in acute coronary syndromes. Int J Cardiol 2012;167:464–9.

9. Fiskesund R, Stegmayr B, Hallmans G, et al. Low levels of antibodies against phosphorylcholine predict development of stroke in a population-based study from Northern Sweden. Stroke 2010;41:607–12.

10. Imhof A, Koenig W, Jaensch A, Mons U, Brenner H, Rothenbacher D. Long-term prognostic value of IgM antibodies against phosphorylcholine for adverse cardiovascular events in patients with stable coronary heart disease. Atherosclerosis 2015;243:414–20.

11. van der Valk FM, Bekkering S, Kroon J, et al. Oxidized phospholipids on lipoprotein(a) elicit arterial wall inflammation and an inflammatory monocyte response in humans. Circulation 2016;134:611–24.

12. Caligiuri G, Khallou-Laschet J, Vandaele M, et al. Phosphorylcholine-targeting immunization reduces atherosclerosis. J Am Coll Cardiol 2007;50:540–6.

13. Binder CJ, Hörkkö S, Dewan A, et al. Pneumococcal vaccination decreases atherosclerotic lesion formation: molecular mimicry between Streptococcus pneumoniae and oxidized LDL. Nat Med 2003;9:736–43.

14. Tsimikas S, Miyanohara A, Hartvigsen K, et al. Human oxidation-specific antibodies reduce foam cell formation and atherosclerosis progression. J Am Coll Cardiol 2011;58:1715–27.

15. Que X, Hung M-Y, Yeang C, et al. Oxidized phospholipids are proinflammatory and proatherogenic in hypercholesterolaemic mice. Nature 2018;558:301–6.

16. Dweck MR, Aikawa E, Newby DE, et al. Noninvasive molecular imaging of disease activity in atherosclerosis. Circ Res 2016;119:330–40.

17. van der Valk FM, Verweij SL, Zwinderman KAH, et al. Thresholds for arterial wall inflammation quantified by 18F-FDG PET imaging: implications for vascular interventional studies. J Am Coll Cardiol Img 2016;9:1198–207.

18. Schindler TH, Schelbert HR, Quercioli A, Dilsizian V. Cardiac PET imaging for the detection and monitoring of coronary artery disease and microvascular health. J Am Coll Cardiol Img 2010;3:623–40.

19. Gupta A, Taqueti V, van de Hoef T, et al. Integrated noninvasive physiological assessment of coronary circulatory function and impact on cardiovascular mortality in patients with stable coronary artery disease. Circulation 2017;136:2325–36.

20. Pettersson K, Ewing MM, de Vries MR, et al. Abstract 15644: A fully human monoclonal IgG phosphorylcholine antibody prevents accelerated atherosclerosis in mice. Circulation 2011;124:A15644.

21. Ewing MM, Karper J, Nordzell M, et al. Chapter 6: Optimizing natural occurring IgM antibodies for therapeutic use: inflammatory vascular disease treatment with anti-phosphorylcholine IgG. Available at: https://openaccess.leidenuniv.nl/

bitstream/handle/1887/21063/06.pdf?sequence=14. Accessed May 21, 2019.

22. Saraste A, Kytö V, Laitinen I, et al. Severe coronary artery stenoses and reduced coronary flow velocity reserve in atherosclerotic mouse model. Doppler echocardiography validation study. Atherosclerosis 2008;200:89–94.

23. Saraste A, Kytö V, Saraste M, Vuorinen T, Hartiala J, Saukko P. Coronary flow reserve and heart failure in experimental coxsackievirus myocarditis. A transthoracic Doppler echocardiography study. Am J Physiol Heart Circ Physiol 2006;291:H871–5.

24. Silvola J, Saraste A, Laitinen I, et al. Effects of age, diet, and type 2 diabetes on the development and FDG uptake of atherosclerotic plaques. J Am Coll Cardiol Img 2011;12:1294–301.

25. Rinne P, Silvola JMU, Hellberg S, et al. Pharmacological activation of the melanocortin system limits plaque inflammation and ameliorates vascular dysfunction in atherosclerotic mice. Arterioscler Thromb Vasc Biol 2014;34:1346–54.

26. Centa M, Jin H, Hofste L, et al. Germinal center-derived antibodies promote atherosclerosis plaque size and stability. Circulation 2019;139:2466–82.

27. Kugiyama K, Kerns SA, Morrisett JD, Roberts R, Henry PD. Impairment of endothelium-dependent arterial relaxation by lysolecithin in modified low-density lipoproteins. Nature 1990;344:160–2.

28. Raitakari OT, Pitkänen OP, Lehtimäki T, et al. In vivo low density lipoprotein oxidation relates to coronary reactivity in young men. J Am Coll Cardiol 1997;30:97–102.

29. Ewing MM, de Vries MR, Nordzell M, et al. Annexin A5 therapy attenuates vascular inflammation and remodeling and improves endothelial function in mice. Arterioscler Thromb Vasc Biol 2011;31:95–101.

30. Tavakoli S, Zamora D, Ullevig S, Asmis R. Bioenergetic profiles diverge during macrophage polarization: implications for the interpretation of ^{18}F-FDG PET imaging of atherosclerosis. J Nucl Med 2013;54:1661–7.

31. Lee SJ, Hoa C, Quach T, et al. Oxidized low-density lipoprotein stimulates macrophage ^{18}F-FDG uptake via hypoxia-inducible factor-1α activation through Nox2-dependent reactive oxygen species generation. J Nucl Med 2016;55:1699–706.

32. Ogawa M, Nakamura S, Saito Y, Kosugi M, Magata Y. What can be seen by F-18-FDG PET in atherosclerosis imaging? The effect of foam cell formation on F-18-FDG uptake to macrophages in vitro. J Nucl Med 2012;53:55–8.

33. Poulsen CB, Al-Mashhadi AL, Von Wachenfeldt K, et al. Treatment with a human recombinant monoclonal IgG antibody against oxidized LDL in atherosclerosis-prone pigs reduces cathepsin S in coronary lesions. Int J Cardiol 2016;215:506–15.

34. Lehrer-Graiwer J, Singh P, Abdelbaky A, et al. FDG-PET imaging for oxidized LDL in stable atherosclerotic disease: a phase II study of safety, tolerability, and anti-inflammatory activity. J Am Coll Cardiol Img 2015;8:493–4.

35. van Dijk RA, Kolodgie F, Ravandi A, et al. Differential expression of oxidation-specific epitopes and apolipoprotein(a) in progressing and ruptured human coronary and carotid atherosclerotic lesions. J Lipid Res 2012;53:2773–90.

36. Witting PK, Pettersson K, Letters J, Stocker R. Site-specific antiatherogenic effect of probucol on apolipoprotein E-deficient mice. Arterioscler Thromb Vasc Biol 2000;20:e26–33.

37. Hellberg S, Sippola S, Liljenbäck H, et al. Effects of atorvastatin and diet interventions on atherosclerotic plaque inflammation and [18F]FDG uptake in Ldlr-/-Apob100/100 mice. Atherosclerosis 2016;263:369–76.

38. Wikström J, Grönros J, Gan LM. Adenosine induces dilation of epicardial coronary arteries in mice: relationship between coronary flow velocity reserve and coronary flow reserve in vivo using transthoracic echocardiography. Ultrasound Med Biol 2008;34:1053–62.

KEY WORDS atherosclerosis, coronary flow reserve, inflammation, ^{18}F-fluorodeoxyglucose positron emission tomography, phosphorylcholine

APPENDIX For expanded Methods and Results sections and supplemental tables and figures, please see the online version of this paper.